Cerebral Cortex November 2008;18:2637–2645
doi:10.1093/cercor/bhn024
Advance Access publication March 4, 2008

Organizational Principles of Human Visual Cortex Revealed by Receptor Mapping

Simon B. Eickhoff[1,2], Claudia Rottschy[1,2], Milenko Kujovic[1], Nicola Palomero-Gallagher[2] and Karl Zilles[1,2,3]

[1]C. & O. Vogt Institute of Brain Research, University of Düsseldorf, Germany, [2]Institute of Neurosciences and Biophysics—Medicine, Research Centre Jülich, Jülich, Germany and [3]Brain Imaging Centre West (BICW), Jülich, Germany

This receptorarchitectonic study of the human visual cortex investigated interareal differences in mean receptor concentrations and laminar distribution patterns of 16 neurotransmitter receptors in the dorsal and ventral parts of areas V1, V2, V3 as well as in adjoining areas V4 (ventrally) and V3A (dorsally). Both the functional hierarchy of these areas and a distinction between dorsal and ventral visual cortices were reflected by significant receptorarchitectonic differences. The observation that dorsoventral differences existed in all extrastriate areas (including V2) is particularly important for the discussion about the relationship between dorsal and ventral V3 as it indicates that a receptorarchitectonic distinction between the ventral and dorsal visual cortices is present in but not specific to V3. This molecular specificity is mirrored by previously reported differences in retinal microstructure and functional differences as revealed in behavioral experiments demonstrating differential advantages for stimulus processing in the upper and lower visual fields. We argue that these anatomical and functional differences may be regarded as the result of an evolutionary optimization adapting to the processing of the most relevant stimuli occurring in the upper and lower visual fields.

Keywords: dorsal, hemifield, hierarchy, retinotopic, stream, ventral

Introduction

The primate visual system comprises numerous cortical areas, which register and process the incoming visual input and forward the computed information to multimodal, cognitive, and motor areas of the cerebral cortex. Within the early visual cortex, the laminar patterns of reciprocal connections (Callaway, 1998; Callaway, 2004; Knierim and Van, 1992) and the increasing computational complexity (Alonso, 2002; Sincich and Horton, 2005) define a hierarchical progression from the primary visual cortex (V1, which receives the vast majority of subcortical input) through adjoining areas V2 and V3 towards higher visual and finally multimodal areas in the posterior parietal and inferior temporal lobes (Kaas and Lyon, 2001; Orban et al., 2004). One of the fundamental organizational principles of at least the early visual cortex is the presence of a retinotopic map within each area containing a representation of the contralateral visual field. Within these maps the lower visual field, i.e., the retinal locations above the horizontal meridian, are represented in the dorsal parts of the visual cortex, whereas the upper visual field is represented ventrally.

It is generally thought that dorsal and ventral parts of V1, that is, containing the representations of the lower and upper hemifields, respectively, form a single homogenous area (Van Essen et al. 2001; Zeki 2003). The same concept is also widely accepted for V2 (Van Essen et al. 2001; Zeki 2003). The relationship between the ventrally located V3v and the dorsally positioned V3d, however, has been a topic of longstanding controversy (Kaas and Lyon 2001; Van Essen et al. 2001; Zeki 2003; Orban et al. 2004). In particular, several authors reported that ventral V3 may be distinct from its dorsal counterpart in terms of its connectivity and functional properties (Burkhalter and Van Essen 1986; Felleman et al. 1997; Tootell et al. 2003). Based on these findings, it has been advocated that V3v should be regarded as a separate area which is distinct from V3d in spite of the single, complete representation of the contralateral hemifield within V3 (Sereno et al. 1995; Shipp et al. 1995). The term VP was hence introduced by some researchers to designate the ventral part of V3. Other groups, however, failed to replicate the findings which have led to the proposition of such a distinct area VP (Lyon and Kaas 2001, 2002; Press et al. 2001; Wade et al. 2002) and conclude the presence of a uniform area V3 with 2 retinotopically defined halves, V3v and V3d. The adjoining areas V4 (located ventrally) and V3A (found dorsally) finally are usually considered distinct and independent of each other (Van Essen et al. 2001; Zeki 2003).

As cortical areas are distinguished by functional and structural criteria (Van Essen et al. 2001; Zeki 2003; Orban et al. 2004), we investigated the molecular correlates of the hierarchical organization as well as the hypothesized distinction between the dorsal and ventral early visual cortex by means of receptor binding site mapping using quantitative in vitro receptor autoradiography.

In particular, this study was aimed at examining the following main questions:

1. Is the hierarchical organization of the human visual cortex reflected by concurrent receptorarchitectonic differences between adjacent areas?
2. Does a neuroanatomical differentiation between upper and lower field representation start at the level of V3 as originally proposed by Burkhalter and Van Essen (1986)? Or does this distinction start no sooner than in the comparison between V3A and V4, supporting the concept of a homogenous area V3 (Zeki 2003)?

Materials and Methods

Four hemispheres (3 right, 1 left) of subjects with no record of neurological or psychiatric diseases were collected under the body donor program of the Department of Anatomy, University of Düsseldorf. Two of the subjects were males, 2 were females; the mean age was 75 years (age range from 72 to 77 years). The post-mortem delay was between 8 and 13 h, which is well within the published limits of sufficient receptor stability (Kontur et al. 1994). Because fixation

Table 1
Overview of neurotransmitter systems, analyzed receptors and tritiated ligands used to label the receptors binding sites (Zilles, Palomero-Gallagher, et al. 2002; Zilles, Schleicher, et al. 2002; Zilles et al. 2004)

System	Receptor	Ligand (c in nM)	K_D	Pharmacology	Displacer (c in nM)	Incubation buffer	Preincubation	Main incubation	Exposure (weeks)
Serotoninergic	5-HT_{1A}	[^{3}H]-8-OH-DPAT (1.0)	2.0	Agonist	5-Hydroxy-tryptamin (10^4)	170 mM Tris–HCl (pH 7.6) + 4 mM $CaCl_2$ + 0.01% ascorbate	30 min, 22 °C	60 min, 22 °C	15
	5-HT_2	[^{3}H]-ketanserin (0.5)	0.5	Antagonist	Mianserin (10^5)	170 mM Tris–HCl (pH 7.7)	30 min, 22 °C	120 min, 22 °C	12
Adrenergic	α_1	[^{3}H]-prazosin (0.2)	0.2	Antagonist	Phentolamine (10^4)	50 mM Tris–HCl (pH 7.4)	30 min, 30 °C	45 min, 30 °C	12
	α_2	[^{3}H]-RX-821002 (6.0)	2.8	Antagonist	Epinephrine–bitartrate (10^4)	50 mM Tris–HCl (pH 7.4) + 1 mM $MgCl_2$ + 0.1% ascorbate	30 min, 22 °C	30 min, 22 °C	18
Glutamatergic	AMPA	^{3}H]-AMPA (10)	10.0	Agonist	Quisqualate (10^4)	50 mM Tris–acetate (pH 7.2) [+100 mM KSCN][a]	30 min, 4 °C	45 min, 4 °C	10
	Kainate	[^{3}H]-kainate (8.0)	12.0	Agonist	Sym 2081 (10^5)	50 mM Tris–citrate (pH 7.1) [+10 mM Ca-acetate][a]	30 min, 4 °C	45 min, 4 °C	10
	NMDA	[^{3}H]-MK-801 (5.0)	5.0	Antagonist	(+)-MK-801 (10^5)	50 mM Tris–HCl (pH 7.2) [+30 AM glycine + 50 AM spermidine][a]	15 min, 22 °C	60 min, 22 °C	10
GABAergic	$GABA_A$	[^{3}H]-muscimol (6.0)	6.0	Agonist	GABA (10^4)	50 mM Tris–citrate (pH 7.0)	15 min, 4 °C	40 min, 4 °C	10
	$GABA_B$	[^{3}H]-CGP 54626 (1.5)	1.48	Antagonist	CGP 55845 (10^5)	50 mM Tris–HCl (pH 7.2)	15 min, 4 °C	60 min, 4 °C	8
	BZ	[^{3}H]-flumazenil	2.0	Antagonist	Clonazepam (2×10^3)	170 mM Tris–HCl (pH: 7.4)	15 min, 4 °C	60 min, 4 °C	10
Cholinergic	M_1	[^{3}H]-pirenzepine (1.0)	3.0	Antagonist	Pirenzepine (2×10^3)	Mod. Krebs-buffer (pH: 7.4)	15 min, 4 °C	60 min, 4 °C	12
	M_2	[^{3}H]-oxotremorine-M (0.8)	0.8	Agonist	Carbachol (10^3)	20 mM HEPES–Tris (pH 7.5) + 10 mM $MgCl_2$	20 min, 22 °C	60 min, 22 °C	12
	M_3	[^{3}H]-4 DAMP (1.0)	1.0	Antagonist	Atropin-sulfate (10^4)	50 mM Tris–HCl (pH: 7.4) + 0.1 mM PSMF + 1 mM ethylenediaminetetraacetic acid	15 min, 22 °C	45 min, 22 °C	15
	Nicotinic ($\alpha4\beta2$)	[^{3}H]-epibatidine (0.5)	0.02	Agonist	(−)Nicotine–hydrogen-tartrate (10^5)	15 mM HEPES–Tris (pH 7.5) + 120 mM NaCl + 5.4 mM KCl + 0.8 mM $MgCl_2$ + 1.8 mM $CaCl_2$	20 min, 22 °C	90 min, 22 °C	15
Dopaminergic	D_1	[^{3}H]-SCH-23390 (0.5)	0.14	Antagonist	SKF 83560 (10^3)	50 mM Tris–HCl (pH 7.4) + 120 mM NaCl + 5 mM KCl + 2 mM $CaCl_2$ + 1 mM $MgCl_2$	20 min, 22 °C	90 min, 22 °C	12
Adenosine (neuromodulator)	A_1	[^{3}H]-cyclopentyl-1,3-dipropylxanthine (4.4)	0.5	Antagonist	R-PIA (10^5)	170 mM Tris–HCl (pH: 7.4) + 2 U/l adenosinedeaminase	15 min, 4 °C	120 min, 22 °C	15

Note: C, concentration; K_D, dissociation constant (population K_d values). DAMP, diphenylacetoxy-N-methylpiperidine methobromide; DPAT, 2-(di-n-propylamino)tetraline; HEPES, 4-(2-hydroxyethyl)-1-piperazineethanesulfonic acid; PMSF, Phenylmethylsulfonylfluorid; R-PIA, R-phenylisopropyladenosine.
[a]Only for main incubation buffer.

would alter structure and hence binding characteristics of receptor molecules, the whole native hemispheres were dissected into 6 slabs, each of which was shock frozen at −40 °C and stored at −70 °C. From these frozen slabs, serial coronal sections (20 μm) were obtained using a large-scale cryostat microtome (Zilles, Palomero-Gallagher, et al. 2002; Zilles, Schleicher, et al. 2002; Zilles et al. 2004) and then alternate sections were incubated with tritiated ligands for 16 different receptors (Table 1) or stained for cell bodies or myelin. The choice of visualized receptors was primarily motivated by our aim to analyze cortical receptorarchitecture. We thus focused on those receptors, whose binding sites are expressed in sufficiently high levels in the cerebral cortex to allow a reliable quantification and preferentially show a regionally differentiated density pattern rather than a homogenous. Importantly, the present analysis included the autoradiographic visualization of receptors for all major classical neurotransmitter systems providing the main substrate of cortical excitation and inhibition. Obviously, the additional analysis of metabotropic receptors or binding sites for nonclassical neurotransmitter/neuromodulators would also provide interesting insight in the organization of the human visual cortex. However, the autoradiographic processing of 16 different receptors in more than a dozen whole hemispheric slices per subject (augmented by cyto- and myeloarchitectonic preparations for each section) is at the currently available technical and logistic limits and makes the applied protocol one of the most extensive set of receptors simultaneously studied using in vitro receptor autoradiography.

Subsequently β-sensitive films (Hyperfilm, Amersham, Piscataway, NJ) were coexposed to the labeled sections and plastic scales of known radioactivity. After developing and digitizing the films, receptor concentrations were measured by using a previously published procedure based on densitometric analysis of the ensuing autoradiographs (Zilles, Palomero-Gallagher, et al. 2002; Zilles, Schleicher, et al. 2002; Zilles et al. 2004). The plastic standards were used to compute a transformation curve representing the relationship between the gray values of the autoradiographs and radioactivity concentrations in the tissue. These concentrations were transformed into maximum binding capacity (B_{max}) values and subsequently into absolute binding site concentrations in fmol/mg protein (Zilles, Palomero-Gallagher, et al. 2002; Zilles, Schleicher, et al. 2002; Zilles et al. 2004). Differences in the dendritic tree of pyramidal neurons in the visual cortex of monkeys have been described (Elston and Rosa 1998; Elston et al. 1999), which may influence the receptor density when referenced against membrane surface and not total protein content as done in the present study. However, there is currently no technique available to quantify the total amount of membrane surface in cortical areas (staining of dendritic trees using SMA-32 or MAP-2 only partially reveal pyramidal dendrites of but not those of interneurons, and provide only qualitative data), the reference of receptor densities to the total amount of protein still remains the gold standard for quantitative receptorarchitectonic analysis and was hence used in the present investigation.

Specificity of binding site densities was evaluated by 2 parallel incubation procedures (Zilles, Palomero-Gallagher, et al. 2002; Zilles, Schleicher, et al. 2002; Zilles et al. 2004). In one of these, the total binding of a given receptor type is visualized by incubating the sections in a solution containing a specific tritiated receptor ligand. In the other, nonspecific binding was determined in adjacent sections by incubation with the tritiated ligand in the presence of the respective unlabeled compound. Because nonspecific binding was clearly less than 5% of the total binding in all cases and receptor types, the total binding was accepted as a good estimate of the specific binding and the respective images were analyzed as described below.

Quantification of Regional and Laminar Receptor Concentrations

The dorsal and ventral parts of areas V1, V2, and V3 as well as areas V3A and V4 were delineated based on contrast-enhanced autoradiographs as well as on observer-independent and microscopic cytoarchitectonic analysis using established criteria (Amunts et al. 2000; Rottschy et al. 2007). Regions of interest (ROIs) were defined for each area on each sectioning level at artifact-free locations (Fig. 1). Because for each rostro-caudal level autoradiography for all 16 receptors, myelin- and cell body stainings were performed on neighboring sections, ROI

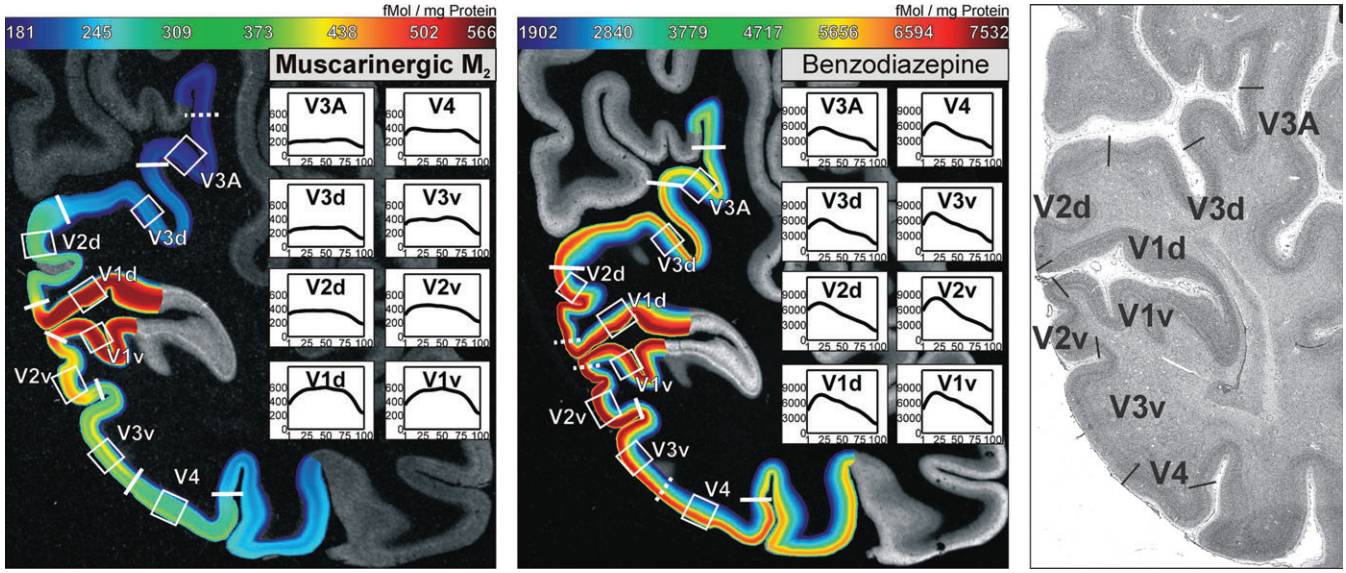

Figure 1. Contrast-enhanced, color-coded autoradiographs for the muscarinic M_2 receptor (left) and the benzodiazepine binding sites (middle). Note that the calcarine section of V1 has not been included in the color coding and smoothing due to its obvious distortions caused by tangentional sectioning of a cortical folding. The location of cytoarchitectonic borders is shown for comparison in panel (right). Cortical areas were defined by receptorarchitectonic differences and cytoarchitectonic examination of adjacent cell body stained sections using quantitative methods (Schleicher et al. 2005) and established anatomical criteria (Amunts et al. 2000; Rottschy et al. 2007). White lines denote the borders between visual areas, whereas the boxes indicate the ROIs, from which receptor density profiles were extracted for all 16 analyzed receptors (Eickhoff, Schleicher, et al. 2007). For illustration, these profiles extracted from this particular section for the adrenergic α_2 receptor are shown in the smaller inserts. Further details and additional examples for this approach are provided by Eickhoff et al. (2007) and Eickhoff, Rottschy, et al. (2007).

delineation could readily be transferred to the individual images (Eickhoff, Schleicher, et al. 2007). From each ROI, a block of 11 adjacent profiles was extracted and averaged to yield a mean receptor density profile for each receptor (Eickhoff, Schleicher, et al. 2007). In total 8–14 ROIs were defined per hemisphere and area, each of which characterized up to 16 (depending on the presence of artifacts and tissue damage) mean receptor density profiles. These profiles were corrected for differences in the relative width of the cortical layers induced by cortical folding using piecewise linear width normalization (Eickhoff, Rottschy, et al. 2007; Eickhoff, Schleicher, et al. 2007), which linearly matches the widths of the individual layer in a ROI to the widths of the mean lamination pattern of the respective area.

Statistical Analysis

Single subject analysis was performed separately for each pair of areas and receptor type by a permutation test (Eickhoff, Schleicher, et al. 2007). First, a mean profile was computed for each area. Dissimilarities in mean receptor concentrations across these profiles were quantified by the asymmetry coefficient (difference between the mean concentrations divided by their sum). Differences in the laminar pattern were quantified by calculating the Euclidean distance between the mean receptor density profiles (consisting of 100 data points each representing the receptor densities at 1–100% cortical depth) after removing effects of absolute concentration (Eickhoff, Rottschy, et al. 2007; Eickhoff, Schleicher, et al. 2007) through division of each profile by its mean: $ED = (\tilde{y}_1 - \tilde{y}_2) * (\tilde{y}_1 - \tilde{y}_2)^T$, where $\tilde{y}_i = \frac{y_i}{\bar{y}_i}$ ($\bar{y}_i$ being the mean receptor density across the profile y_i of receptor concentrations). Subsequently, the profiles sampled for both areas were randomly reassigned into 2 groups, averaged, and the calculation of the distance measures was repeated. That is, the differences in mean concentration and laminar distribution pattern were computed between groups randomly containing profiles from both areas. One hundred thousand iterations of those random reassignments yielded the null distribution for statistical evaluation of the observed (true) differences. Given this null hypothesis, the *P*-value associated with a specific difference observed in the comparison of interest is equal to the proportion of randomly assembled groups showing the same or a more extreme value.

Due to the small sample sizes available for receptorautoradiographic analysis, group inference was performed via a multisubject conjunction analysis (Eickhoff, Schleicher, et al. 2007). It has been shown (Friston et al. 2005; Nichols et al. 2005), that valid conjunction analyses across subjects is best computed (for a specific comparison v within a set of V simultaneous comparisons) via the corresponding minimum statistic ($M_{(v)}$), corresponding to the maximum *P*-value for the K subjects in our nonparametric analysis. This minimum statistic represented the test statistic for the conjunction analysis, which is declared significant, if $M_{(v)}$ was lower than a threshold α_0. This threshold was adjusted such as to control the family-wise error rate α_{FWE} of the whole analysis to ensure that the probability of obtaining one or more false positive results was less than $\alpha_{FWE} = 0.05$. The threshold α_0 needed to control for a specified family-wise error rate can be derived from the required corrected significance level by $\alpha_0 = (1-(1-a_{FWR})^{1/V})^{1/K}$ (Nichols et al. 2005; Eickhoff, Schleicher, et al. 2007).

Results

The dorsal and ventral parts of V1, V2, and V3 as well as areas V4 and V3A (Fig. 1) were identified using established cytoarchitectonic criteria (Amunts et al. 2000; Rottschy et al. 2007) and the contrast-enhanced, color-coded autoradiographic images in which areal borders can be identified based on changes in receptor density or distribution (Fig. 1, cf. Eickhoff Rottschy et al. 2007). Receptor density profiles were subsequently extracted from 8-14 regions of interest (per case) within these areas to quantify the mean concentrations and the laminar distribution pattern (cf. supplementary material, Figures S1-S3) of neurotransmitter receptors within the human early visual cortex. The differences in cortical receptor density and distribution were then analysed between each area and its neighbours as well as between the dorsal and ventral counterparts of a given area (Fig. 2).

Receptorarchitectonic Differences Reflecting Cortical Hierarchy

Several receptors showed concurrent increases or decreases in mean binding site concentrations in both the dorsal and ventral

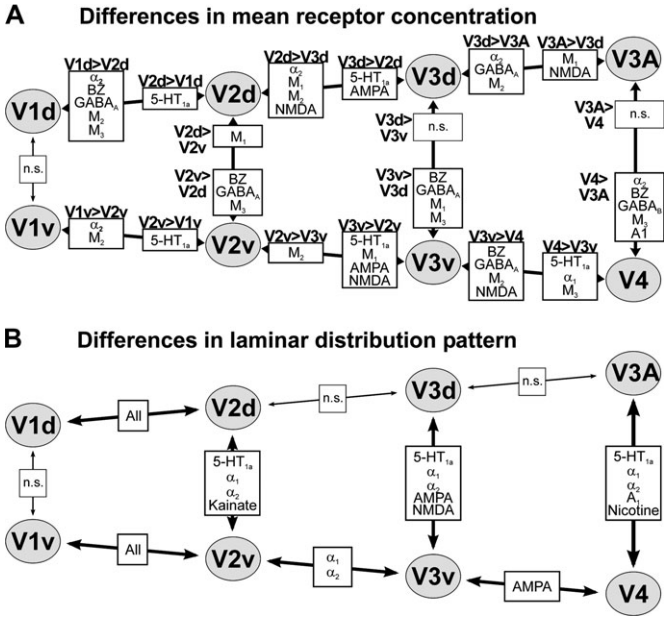

Figure 2. Significant ($P < 0,05$, family-wise error corrected) differences in mean receptor concentration (*A*) or laminar receptor distribution pattern (*B*) between visual areas, which are either adjacent or corresponding to each other in the retinotopic organization of early visual cortex.

parts of the analyzed areas reflecting subsequent steps of the cortical hierarchy. In particular, the progression from V1 to V2, V3, and finally to V4/V3A was characterized by a significant increase in serotoninergic 5-hydroxytryptophan $(5\text{-HT})_{1A}$ receptor densities from less than 200 fmol/mg protein in V1 to approximately 400 fmol/mg protein in V4 and V3A (Fig. 3*A*). In contrast, binding site densities of the muscarinic cholinergic M_2 receptor binding sites were highest in the primary visual cortex and decreased with the progression toward hierarchically higher areas (Figs 2*A*, 3*A*). The densities of the noradrenergic α_2 receptors were also significantly higher in V1d and V1v than in V2d and V2v, respectively. However, whereas the concentrations M_2 receptors showed a further significant decline in both the ventral and the dorsal visual cortices, the α_2 receptor showed further decreases of receptor concentration only in the dorsal areas, that is between V2d and V3d and between V3d and V3A (Figs 2*A*, 3*A*). Several other receptors also feature differences in both ventral and dorsal visual cortices reflecting individual steps of the hierarchical progression in the visual cortex. In particular, the concentrations of the glutamatergic AMPA receptor showed a significant increase from V2v/V2d to V3v/V3d, respectively, and hence marked the transition between the second and the third visual area. The $GABA_A$ receptor, whose concentrations were significantly lower in V4 and V3A, as compared with V3v and V3d, respectively (Fig. 2*A*, cf. Fig. 3*B*) revealed the subsequent step of the cortical hierarchy. Finally, NMDA receptors were found with significantly higher concentrations in V3v as compared with the neighboring areas V2v and V4, whereas their concentration was significantly lower in V3d as compared with the adjacent areas V2d and V3A.

Differences in laminar receptor distribution patterns between hierarchically adjacent areas, however, were primarily observed when comparing V1v to V2v and V1d to V2d (Fig. 2*B*), where all analyzed receptors showed a significant change in laminar pattern. Differences in laminar distribution pattern corresponding to the hierarchical progression within the extrastriate cortex, on the other hand, were sparse. V2v and V3v differed in the laminar distribution of both analyzed adrenergic receptors (α_1 and α_2), whereas V3v and V4 showed a different laminar distribution of AMPA binding sites.

Receptorarchitectonic Differences between Dorsal and Ventral Visual Cortex

The ventral (V1v) and dorsal (V1d) parts the of primary visual cortex did not differ significantly from each other with respect to the mean binding site densities (averaged over all cortical layers) or the laminar distribution patterns of any examined receptor (Fig. 2*A*). In contrast to these findings in the striate cortex, several receptors were identified which showed consistent differences between the ventral and dorsal counterparts of the analyzed extrastriate areas. In particular, differences between the dorsal and ventral parts of V2 and V3, as well as those between V4 and V3A, were characterized by significantly higher densities of M_3 receptors and benzodiazepine binding sites in the ventrally located areas (Figs 2*A*, 3*B*).

In addition to the M_3 receptors and the benzodiazepine binding sites, which showed a dorsoventral asymmetry throughout the entire extrastriate cortex, the ventral parts of V2 and V3 also showed significantly higher $GABA_A$ concentrations than their dorsal counterparts (Figs 2*A*, 3*B*). Moreover, $GABA_A$ receptors also showed a nonsignificant trend to higher concentration in V4 as compared with V3A. These 2 areas (V4 and V3A), however, showed a significant difference in mean $GABA_B$ and A_1 receptor densities, which were both found more frequently in the ventral visual cortex. The only comparison between ventral and dorsal visual areas in which significantly higher receptor concentrations were observed dorsally related to the M_1 receptor densities within V2. Notably, however, the same receptor (M_1) showed significantly higher concentrations in the ventral part of area V3.

In contrast to the observation that differences in laminar distribution patterns between hierarchically adjacent areas were only sparsely present in the extrastriate cortex (Fig. 2*B*), we found that 3 of the examined receptors show consistent differences in laminar pattern between ventral and dorsal parts of areas V2 and V3 as well as between V4 and V3A. The 5-HT_{1A} receptor showed very low relative concentrations in deeper cortical layers (V–VI) of the dorsal visual areas (V2d, V3d, and V3A), which were higher in their ventral counterparts (V2v, V3v, and V4). The α_1 receptor likewise showed higher concentration in the lower cortical layers in the ventral visual cortex and in addition also a less pronounced peak in relative receptor concentration at the border between layers I and II ventrally. The third receptor to feature consistent differences was the α_2 receptor, for which a peaks of high receptor concentrations in layer I were only observed for the dorsal extrastriate cortex. Finally, all 3 analyzed glutamatergic receptors also showed significant dorsoventral differences in laminar pattern. Kainate receptors were found with higher relative concentrations in the infragranular layers of the dorsal part of V2, AMPA binding sites showed a more superficial location of its density peak in V3d as compared with V3v and NMDA receptors lower concentrations in layer II/III in V3v.

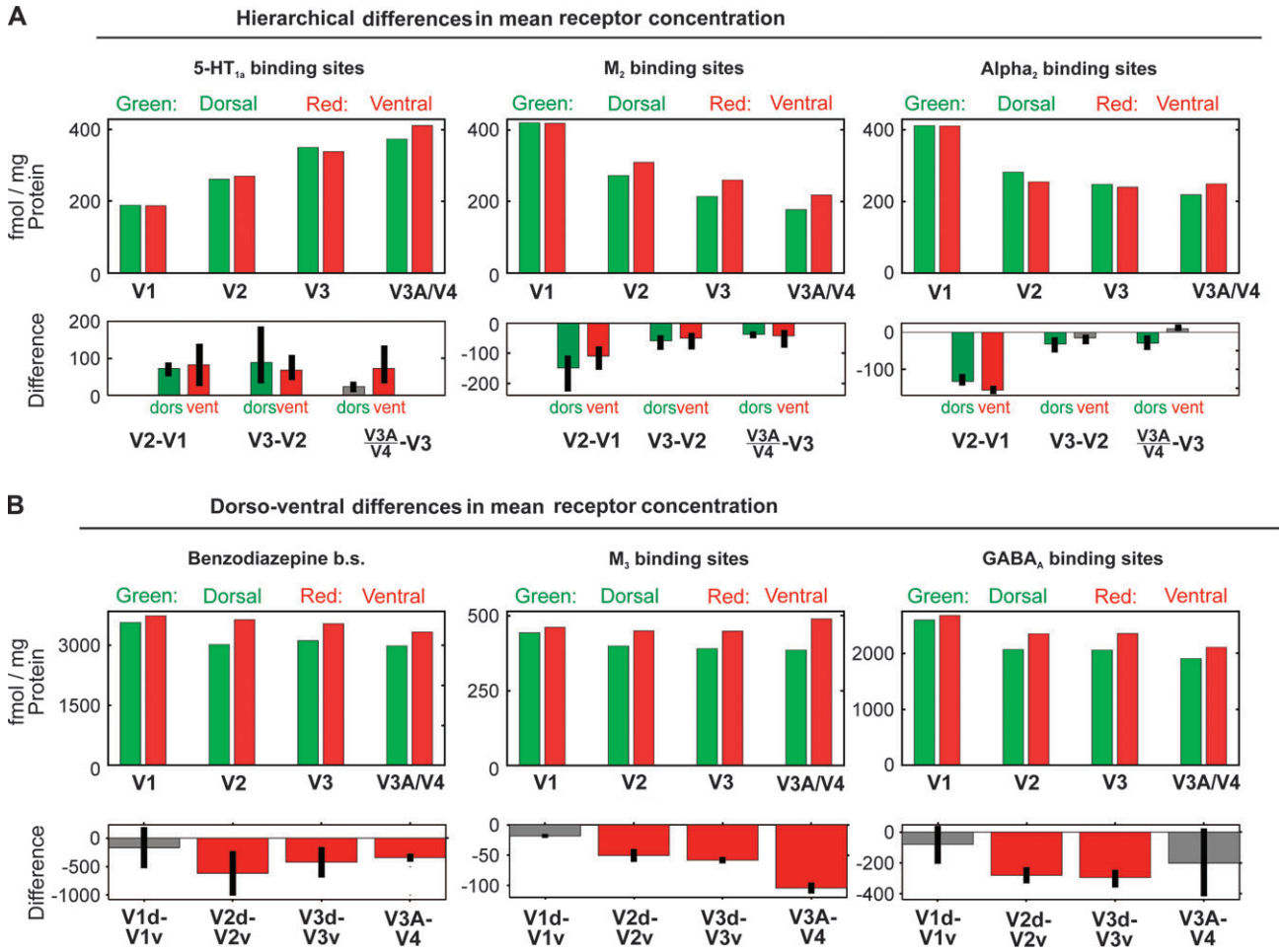

Figure 3. Synopsis of the mean concentrations for those receptors, which showed consistent differences reflecting cortical hierarchy (*A*) or visual stream distinction (*B*). All bars represent grand mean concentrations obtained from averaging the mean (across ROIs) concentrations of the 4 individual cases. The lower rows give the mean difference between hierarchically adjacent (*A*, separately by visual stream), respectively, corresponding areas (*B*). Significant differences are shown by colored bars, nonsignificant ones in gray. Lines denote the minimum and maximum difference observed in individual cases. Because the statistical analysis was carried out as a conjunction requiring significant effects in each case, these lines do not implicate statistical significance. Confidence intervals, however, would contradict the logic of multisubject conjunction studies needed to analyze the small sample sizes available for autoradiographic data.

Discussion

In this study we analyzed the distribution of 16 neurotransmitter receptors in visual areas V1, V2, V3, and V4/V3A by quantitative in vitro autoradiography (Eickhoff, Rottschy, et al. 2007; Eickhoff, Schleicher, et al. 2007). Importantly, whereas receptorarchitectonic studies on the visual cortex of primates have already been reported (Rakic et al. 1988; Lidow et al. 1989), the present study is the first to investigate the receptorarchitectonic organization of its first 4 hierarchical levels separately for their dorsal respectively components allowing new insights in the relationship between these.

Receptorarchitectonic Correlates of Hierarchical Organization

5-HT_{1A} and M_2 receptors showed significant changes in mean concentrations when moving from V1 to V2, V3 and V4/V3A, indicative of a monotonic hierarchical progression throughout the early visual cortex (Felleman and Van Essen 1991; Orban et al. 2004; Zeki and Shipp 1988). Others receptorarchitectonic changes, however, were specific to a particular hierarchical level (AMPA increasing from V2 to V3, $GABA_A$ decreasing beyond V3) indicating discontinuous changes. These may be regarded as potential anatomical correlates of the functional differences between the analysed areas, although the contribution of different aspects of cortical circuitry (connectivity, CO patterns, cyto- and receptorarchitecture) to the functional specialisation of cortical areas, e.g., the local integration of line elements in V1 and V2 (Kourtzi et al. 2003) or the involvement of V2 and V3 in the extraction of 3D-structure from motion (Vanduffel et al. 2002), is yet unclear. Considerable potential for the further investigation of these issues may lie in the combination of functional imaging data with probabilistic cytoarchitectonic maps (Eickhoff, Stephan, et al. 2005; Eickhoff, Paus, et al. 2007) of those visual areas (Amunts et al. 2000; Rottschy et al. 2007) for which receptorarchitectonic data is now reported. Differences in laminar distribution pattern, however, were only observed between coniocortical area V1 and isocortical V2, reflecting the specialized architecture of the striate cortex (Horton and Hocking 1997; Amunts et al. 2000; Eickhoff, Walters, et al. 2005).

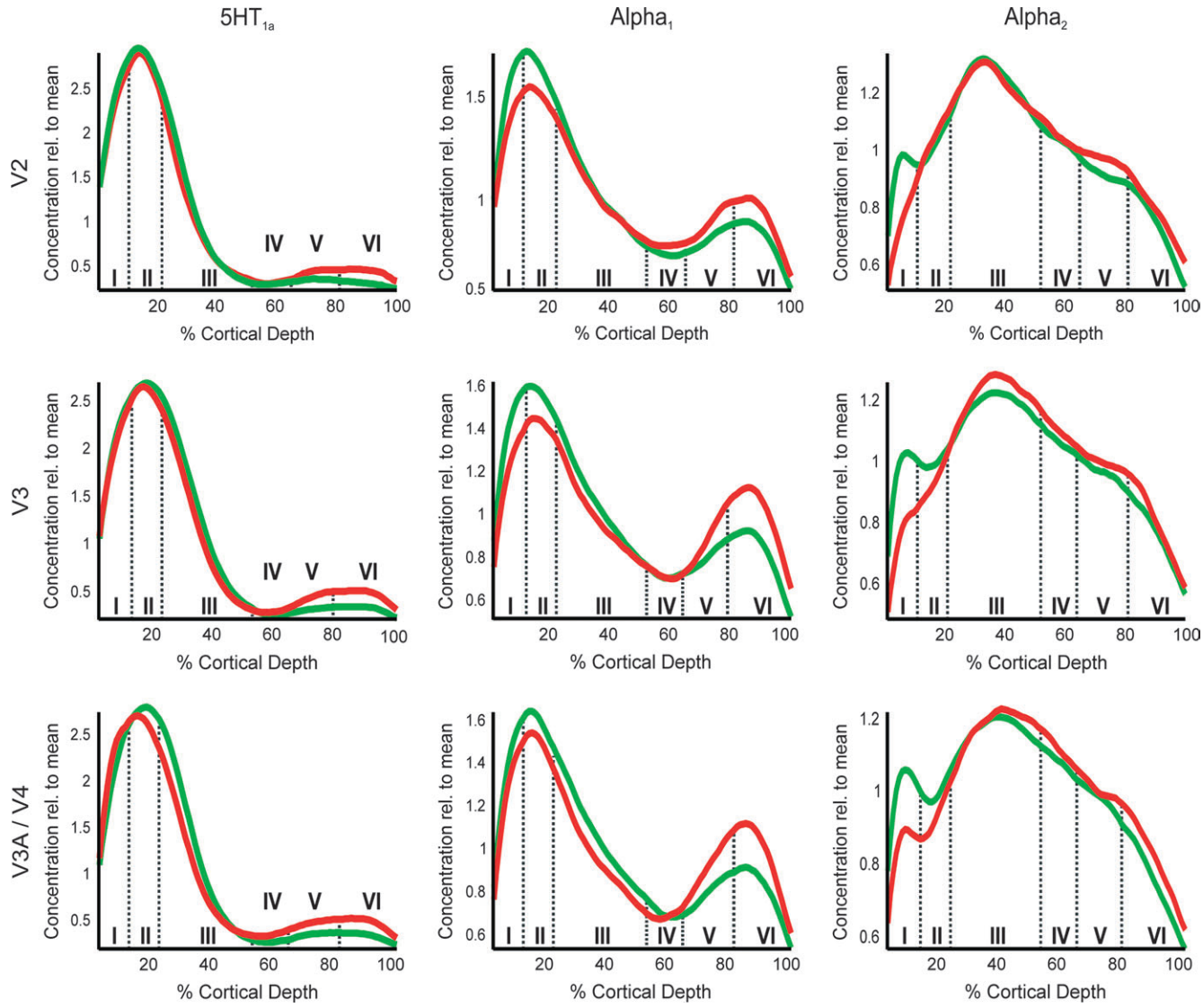

Figure 4. Laminar distribution patterns in ventral/dorsal V2 and V3 as well as V4/V3A for those receptors, showing consistent laminar differences between both visual streams (cf. Fig. 2). All displayed profiles are grand mean profiles obtained from averaging the mean (across ROIs) profiles of the 4 individual cases analyzed in this study.

Relation of Measurement Sites to Retinotopic Representations

Measurements within V1v - V3v should correspond to regions processing the upper hemifield, while V1d - V3d reflect areas involved in lower field processing (Hansen et al. 2007). The organisation of the cortex lateral to V3v, the "V4 region" certainly shows a complex organisation for which various concepts have been presented (Hadjikhani et al. 1998; Hansen et al. 2007 Larsson and Heeger, 2006; Press et al. 2001; Wandell et al. 2005). In spite of the differences in the proposed organisation of more anterior, lateral or dorsal parts of this region, all authors, however, agree on the fact that the cortex immediately adjacent to V3v contains a representation of the lower visual field. It thus seems likely that the receptorarchitectonic measurements within "V4" as anatomically defined in the present study, which were located close to the border with area V3v sample cortex involved in upper visual field processing similar to V2v and V3v. The cortex immediately adjacent to area V3d (anatomical area "V3A") was shown to contain a lower field representation, which is subsequently followed by representation of the upper visual field (Hansen et al. 2007; Larsson and Heeger 2006; Press et al. 2001; Wandell et al. 2005). Consequently, we may assume that the receptorarchitectonic measurements designated as "V3A" should most likely correspond to portions of the cortex devoted to lower visual field processing in a similar fashion to the measurements within areas V3d and V2d.

Relationship between Dorsal and Ventral Parts of the Early Visual Cortex

Our results shed a new light on the controversy about the relationship between dorsal and ventral V3 (Kaas and Lyon 2001; Van Essen et al. 2001; Zeki 2003; Orban et al. 2004). Based on studies in nonhuman primates, it has been suggested that the ventral part of V3 distinct from its dorsal counterpart in terms of function and connectivity and should accordingly be considered a separate area, VP (Burkhalter and Van Essen 1986; Felleman et al. 1997; Van Essen et al. 2001; Orban et al.

2004). Other groups did not replicate these differences (Rosa et al. 2000; Lyon and Kaas 2002; Wade et al. 2002) and argued that a distinction into V3 and VP would contrast to the single complete visual field representation shared by V3v/V3d (Kaas and Lyon 2001; Zeki 2003) which is comparable to V2 or V1, where dorsal and ventral parts are considered to constitute a single area (Van Essen et al. 2001; Zeki 2003).

Based on these 2 concepts we hypothesized a receptorarchitectonic distinction between dorsal and ventral areas to emerge either at the level of V3, in line with the distinction into V3d and V3v/VP proposed by Burkhalter and Van Essen (1986) or no sooner than in the comparison of V4/V3A, reflecting a homogenous area V3 (Lyon and Kaas 2002; Zeki 2003). The results of our statistical analysis, however, do not support either view. Corresponding to the proposed distinction between V3d and VP, we observed differences in receptor distribution between dorsal and ventral V3. However, the same anatomical differences were also evident between the dorsal and ventral parts of V2. That is, contradicting the "VP concept", our data does not indicate a fundamental distinction between a homogenous area V2 on one side, and 2 separate areas V3 and VP on the other. At the same time, though, the clear architectonic differences within V2 and V3 also disagree with the view that both are homogenous areas within which dorsal and ventral parts only differ by retinotopic preference.

Based on the regional distribution of neurotransmitter receptors we would therefore propose a revised model for the organization of the early extrastriate cortex, in which the undisputed hierarchical difference between V2 and V3 is augmented by a distinction between the dorsal and ventral parts of these areas, that is, their upper and lower field representations. This dorsoventral asymmetry is then continued within the presumed upper and lower field representations of the subsequent areas V3A and V4.

Dorsoventral Asymmetries within the Visual System

Although being unaccounted for in the current concepts of visual cortex organization, the observed differences between upper and lower field representation within the entire early extrastriate cortex concur with previous reports on differences in the neural substrates for processing information from either hemifield. This divergence starts already in the retina, where histological studies have reported reliable dorsoventral asymmetries. In particular the retinas of both humans and nonhuman primates show an inhomogeneous distribution of regional cone and rod densities (Packer et al. 1989; Curcio et al. 1990; Wikler et al. 1990; Andrade da Costa and Hokoc 2000). At equivalent eccentricities cones are found in higher densities in the superior part of the retina, which receives the input from the lower part of the visual field, as compared with its inferior portion covering the upper visual field. In contrast, the density of rods, in particular in the "rod ring" at the eccentricity of the optic disk is considerably higher in the inferior part of the retina. Moreover, it has been shown (Curcio and Allen 1990), that the ganglion cell densities is up to 60% higher within the superior part of the human retina. Finally, in many species featuring a tapetum lucidum (a reflecting layer immediately behind the retina reflecting light back to the photoreceptors) this structure is either less developed or even absent in the inferior retina (Chijiiwa et al. 1990; Ollivier et al. 2004).

Although differences between upper and lower visual field representations within the superior colliculus or the lateral geniculate nucleus have, to our knowledge, not yet been reported, a diverging architecture of the stripe-subsystem defined by histochemical staining for cytocrome oxidase between the dorsal and ventral aspect of V2 has already been reported (Olavarria and Van Essen 1997). Unfortunately, a further investigation on the receptorarchitectonic correlates of these stripes and the blob–interblob subsystems within V1, which are considered to form parallel streams of V1 to V2 connectivity mediating different aspects of visual perception (Sincich and Horton 2005), was not possible in the current study. Both systems are reliably identifiable only in physically unfolded and flattened specimen, the present study, however, was performed—as part of a whole-brain mapping project—on thin coronal sections through the occipital lobe.

Importantly, these anatomical differences seem to impact the efficiency with which different aspects of visual input is analyzed, as there is a considerable amount of behavioral studies showing differential advantages for visual processing between the lower and upper hemifield. For example, the lower visual field was reported to have advantages in tasks such as visuomotor feedback processing (Khan and Lawrence 2005), visually guided pointing (Danckert and Goodale 2001) and spatial relocation memory (Genzano et al. 2001). In contrast, the upper hemifield seems to be advantageous, for example, for stimuli discrimination (Levine and McAnany 2005) and change detection (Rutkowski et al. 2002).

Conclusions

Apart from identifying the receptorarchitectonic correlates of the hierarchical organization within the early visual cortex, this study demonstrated consistent dorsoventral asymmetries within V2 and V3, which contrast with both contemporary concepts about the organization of the early extrastriate cortex (Van Essen et al. 2001; Zeki 2003). Rather, in combination with previously reported functional and anatomical asymmetries they point to a generalized distinction between the neuronal substrates for upper versus lower visual field representation, possibly representing an evolutionary adaptation for processing the most relevant stimuli in each hemifield: Due to the caudal location of the hands, eye-hand coordination will mainly take place in the lower visual field represented in the dorsal visual cortex, whereas visual exploration of larger scenes will predominantly be occurring in the upper visual field, that is, the ventral visual cortex.

Funding

National Institute of Biomedical Imaging and Bioengineering; National Institute of Neurological Disorders and Stroke; National Institute of Mental Health; and Deutsche Forschungsgemeinschaft (KFO-112) funded the Human Brain Project/Neuroinformatics research.

Notes

We would like to thank A. Schleicher for valuable advice and support, G. Plant for insightful discussions as well as R. Dohm and N. Dechering for their excellent technical assistance. *Conflict of Interest*: None declared.

Address correspondence to Simon Eickhoff, MD, Institut of Institute of Neurosciences and Biophysics (IME), Forschungszentrum Jülich GmbH, D-52425 Jülich, Germany. Email: S.Eickhoff@fz-juelich.de.

References

Alonso JM. 2002. Neural connections and receptive field properties in the primary visual cortex. Neuroscientist. 8:443–456.

Amunts K, Malikovic A, Mohlberg H, Schormann T, Zilles K. 2000. Brodmann's areas 17 and 18 brought into stereotaxic space—where and how variable? Neuroimage. 11:66–84.

Andrade da Costa BL, Hokoc JN. 2000. Photoreceptor topography of the retina in the New World monkey Cebus apella. Vision Res. 40:2395–2409.

Burkhalter A, Van Essen DC. 1986. Processing of color, form and disparity information in visual areas VP and V2 of ventral extrastriate cortex in the macaque monkey. J Neurosci. 6:2327–2351.

Callaway EM. 1998. Local circuits in primary visual cortex of the macaque monkey. Annu Rev Neurosci. 21:47–74.

Callaway EM. 2004. Feedforward, feedback and inhibitory connections in primate visual cortex. Neural Netw. 17:625–632.

Chijiiwa T, Ishibashi T, Inomata H. 1990. Histological study of choroidal melanocytes in animals with tapetum lucidum cellulosum. Graefes Arch Clin Exp Ophthalmol. 228:161–168.

Curcio CA, Allen KA. 1990. Topography of ganglion cells in human retina. J Comp Neurol. 300:5–25.

Curcio CA, Sloan KR, Kalina RE, Hendrickson AE. 1990. Human photoreceptor topography. J Comp Neurol. 292:497–523.

Danckert J, Goodale MA. 2001. Superior performance for visually guided pointing in the lower visual field. Exp Brain Res. 137:303–308.

Eickhoff SB, Paus T, Caspers S, Grosbas MH, Evans AC, Zilles K, Amunts K. 2007. Assignment of functional activations to probabilistic cytoarchitectonic areas revisited. Neuroimage. 36:511–521.

Eickhoff SB, Rottschy C, Zilles K. 2007. Laminar distribution and co-distribution of neurotransmitter receptors in early human visual cortex. Brain Struct Funct. 212:255–267.

Eickhoff SB, Schleicher A, Scheperjans F, Palomero-Gallagher N, Zilles K. 2007. Analysis of neurotransmitter receptor distribution patterns in the cerebral cortex. Neuroimage. 34:1317–1330.

Eickhoff SB, Stephan KE, Mohlberg H, Grefkes C, Fink GR, Amunts K, Zilles K. 2005. A new SPM toolbox for combining probabilistic cytoarchitectonic maps and functional imaging data. Neuroimage. 25:1325–1335.

Eickhoff S, Walters NB, Schleicher A, Kril J, Egan GF, Zilles K, Watson JD, Amunts K. 2005. High-resolution MRI reflects myeloarchitecture and cytoarchitecture of human cerebral cortex. Hum Brain Mapp. 24:206–215.

Elston GN, Rosa MG. 1998. Morphological variation of layer III pyramidal neurones in the occipitotemporal pathway of the macaque monkey visual cortex. Cereb Cortex. 8:278–294.

Elston GN, Tweedale R, Rosa MG. 1999. Cortical integration in the visual system of the macaque monkey: large-scale morphological differences in the pyramidal neurons in the occipital, parietal and temporal lobes. Proc Biol Sci. 266:1367–1374.

Felleman DJ, Burkhalter A, Van E. 1997. Cortical connections of areas V3 and VP of macaque monkey extrastriate visual cortex. J Comp Neurol. 379:21–47.

Felleman DJ, Van Essen DC. 1991. Distributed hierarchical processing in the primate cerebral cortex. Cereb Cortex. 1:1–47.

Friston KJ, Penny WD, Glaser DE. 2005. Conjunction revisited. Neuroimage. 25:661–667.

Genzano VR, Di NF, Ferlazzo F. 2001. Upper/lower visual field asymmetry on a spatial relocation memory task. Neuroreport. 12:1227–1230.

Hadjikhani N, Liu AK, Dale AM, Cavanagh P, Tootell RB. 1998. Retinotopy and color sensitivity in human visual cortical area V8. Nat Neurosci. 1:235–241.

Hansen KA, Kay KN, Gallant JL. 2007. Topographic organization in and near human visual area V4. J Neurosci. 27:11896–11911.

Horton JC, Hocking DR. 1997. Myelin patterns in V1 and V2 of normal and monocularly enucleated monkeys. Cereb Cortex. 7:166–177.

Kaas JH, Lyon DC. 2001. Visual cortex organization in primates: theories of V3 and adjoining visual areas. Prog Brain Res. 134:285–295.

Khan MA, Lawrence GP. 2005. Differences in visuomotor control between the upper and lower visual fields. Exp Brain Res. 164:395–398.

Knierim JJ, Van E. 1992. Visual cortex: cartography, connectivity, and concurrent processing. Current Opinion in Neurobiology. 2:150–155.

Kontur PJ, al Tikriti M, Innis RB, Roth RH. 1994. Postmortem stability of monoamines, their metabolites, and receptor binding in rat brain regions. J Neurochem. 62:282–290.

Kourtzi Z, Tolias AS, Altmann CF, Augath M, Logothetis NK. 2003. Integration of local features into global shapes: monkey and human FMRI studies. Neuron. 37:333–346.

Larsson J, Heeger DJ. 2006. Two retinotopic visual areas in human lateral occipital cortex. J Neurosci. 26:13128–13142.

Levine MW, McAnany JJ. 2005. The relative capabilities of the upper and lower visual hemifields. Vision Res. 45:2820–2830.

Lidow MS, Gallager DW, Rakic P, Goldman-Rakic PS. 1989. Regional differences in the distribution of muscarinic cholinergic receptors in the macaque cerebral cortex. J Comp Neurol. 289:247–259.

Lyon DC, Kaas JH. 2001. Connectional and architectonic evidence for dorsal and ventral V3, and dorsomedial area in marmoset monkeys. J Neurosci. 21:249–261.

Lyon DC, Kaas JH. 2002. Evidence for a modified V3 with dorsal and ventral halves in macaque monkeys. Neuron. 33:453–461.

Nichols T, Brett M, Andersson J, Wager T, Poline JB. 2005. Valid conjunction inference with the minimum statistic. Neuroimage. 25:653–660.

Olavarria JF, Van Essen DC. 1997. The global pattern of cytochrome oxidase stripes in visual area V2 of the macaque monkey. Cereb Cortex. 7:395–404.

Ollivier FJ, Samuelson DA, Brooks DE, Lewis PA, Kallberg ME, Komaromy AM. 2004. Comparative morphology of the tapetum lucidum (among selected species). Vet Ophthalmol. 7:11–22.

Orban GA, Van ED, Vanduffel W. 2004. Comparative mapping of higher visual areas in monkeys and humans. Trends Cogn Sci. 8:315–324.

Packer O, Hendrickson AE, Curcio CA. 1989. Photoreceptor topography of the retina in the adult pigtail macaque (Macaca nemestrina). J Comp Neurol. 288:165–183.

Press WA, Brewer AA, Dougherty RF, Wade AR, Wandell BA. 2001. Visual areas and spatial summation in human visual cortex. Vision Res. 41:1321–1332.

Rakic P, Goldman-Rakic PS, Gallager D. 1988. Quantitative autoradiography of major neurotransmitter receptors in the monkey striate and extrastriate cortex. J Neurosci. 8:3670–3690.

Rosa MG, Pinon MC, Gattass R, Sousa AP. 2000. "Third tier" ventral extrastriate cortex in the New World monkey, Cebus apella. Exp Brain Res. 132:287–305.

Rottschy C, Eickhoff SB, Schleicher A, Mohlberg H, Kujovic M, Zilles K, Amunts K. 2007. The ventral visual cortex in humans: cytoarchitectonic mapping of two extrastriate areas. Hum Brain Mapp. 212:255–267.

Rutkowski JS, Crewther DP, Crewther SG. 2002. Normal readers have an upper visual field advantage in change detection. Clin Exp Ophthalmol. 30:227–330.

Schleicher A, Palomero-Gallagher N, Morosan P, Eickhoff SB, Kowalski T, de Vos K, Amunts K, Zilles K. 2005. Quantitative architectural analysis: a new approach to cortical mapping. Anat Embryol (Berl). 210:373–386.

Sereno MI, Dale AM, Reppas JB, Kwong KK, Belliveau JW, Brady TJ, Rosen BR, Tootell RB. 1995. Borders of multiple visual areas in humans revealed by functional magnetic resonance imaging. Science. 268:889–893.

Shipp S, Watson JD, Frackowiak RS, Zeki S. 1995. Retinotopic maps in human prestriate visual cortex: the demarcation of areas V2 and V3. Neuroimage. 2:125–132.

Sincich LC, Horton JC. 2005. The circuitry of V1 and V2: integration of color, form, and motion. Annu Rev Neurosci. 28:303–326.

Tootell RB, Tsao D, Vanduffel W. 2003. Neuroimaging weighs in: humans meet macaques in "primate" visual cortex. J Neurosci. 23:3981–3989.

Van Essen DC, Lewis JW, Drury HA, Hadjikhani N, Tootell RB, Bakircioglu M, Miller MI. 2001. Mapping visual cortex in monkeys and humans using surface-based atlases. Vision Res. 41:1359–1378.

Vanduffel W, Fize D, Peuskens H, Denys K, Sunaert S, Todd JT, Orban GA. 2002. Extracting 3D from motion: differences in human and monkey intraparietal cortex. Science. 298:413–415.

Wade AR, Brewer AA, Rieger JW, Wandell BA. 2002. Functional measurements of human ventral occipital cortex: retinotopy and colour. Philos Trans R Soc Lond B Biol Sci. 357:963–973.

Wandell BA, Brewer AA, Dougherty RF. 2005. Visual field map clusters in human cortex. Philos Trans R Soc Lond B Biol Sci. 360:693–707.

Wikler KC, Williams RW, Rakic P. 1990. Photoreceptor mosaic: number and distribution of rods and cones in the rhesus monkey retina. J Comp Neurol. 297:499–508.

Zeki S. 2003. Improbable areas in the visual brain. Trends Neurosci. 26:23–26.

Zeki S, Shipp S. 1988. The functional logic of cortical connections. Nature. 335:311–317.

Zilles K, Palomero-Gallagher N, Grefkes C, Scheperjans F, Boy C, Amunts K, Schleicher A. 2002. Architectonics of the human cerebral cortex and transmitter receptor fingerprints: reconciling functional neuroanatomy and neurochemistry. Eur Neuropsychopharmacol. 12:587–599.

Zilles K, Palomero-Gallagher N, Schleicher A. 2004. Transmitter receptors and functional anatomy of the cerebral cortex. J Anat. 205:417–432.

Zilles K, Schleicher A, Palomero-Gallagher N, Amunts K. 2002. Quantitative analysis of cyto- and receptor architecture of the human brain. In: Mazziotta J, Toga A, editors. Brain mapping, the methods. Amsterdam, The Netherlands: Elsevier. p. 573–602.